

Structural Chemistry

Numerous important solid-state structures can be described by *eutactic* (close packed) arrangements of atoms with other atoms occupying the void spaces. However, this description is a purely geometrical perspective of structure and provides no clear rationales based on the characteristics and relative quantities of the elemental components. From a chemical perspective, valence electron counting can account for numerous local environments in solids. For example, the Valence State Electron Pair Repulsion (VSEPR) model rationalizes local coordination geometries at *p*-elements and the octet rule aptly describes their connectivities in extended solids, like Zintl phases. Wade-Lipscomb rules are useful when structures contain clusters of main group elements. And, determining *d*-electron configurations of transition metals from their oxidation states can explain ligand coordination geometries and the possibilities of metal-metal bonding. In general, combining valence electron counting procedures with analyses of atomic sizes and electronegativities can effectively rationalize many solid-state structures. If certain structural subtleties appear, then some form of computational work, whether using electronic structure theory or interatomic pair potentials, is usually warranted for an in-depth understanding of experimental observations.

READING: A.F. Wells, *Structural Inorganic Chemistry*, 5th Ed., pp. 161-176, 179-186, 238-273, 578-589;

H.F. Franzen, *Physical Chemistry of Inorganic Crystalline Solids*, pp. 37-57, 124-130;

J.K. Burdett, *Chemical Bonding in Solids*, pp. 219-269.

(41) Eutactic Structures: Idealized eutactic arrangements of atoms such as HCP, CCP, and their mixtures create one octahedral and two tetrahedral voids per atom. Many different structures can be created by filling various fractions of each type of void either separately or in combination. The patterns of filling these voids depend on various characteristics of the different components, as mentioned above, such as valence electron count and their relative electronegativities and sizes. One important “guiding principle”, sometimes cited as Pauling’s third rule for ionic compounds, is: “*The existence of edges and particularly of faces, common to two anion polyhedra in a coordinated structure decreases its stability; this effect is large for cations with high valency and small coordination number and is especially large when the radius ratio approaches the lower limit of stability of the polyhedra*” (see Burdett, pp. 191-218). A consequence of this “rule” is that the filling patterns of octahedra and/or tetrahedra in eutactic packings tend to avoid sharing faces. In particular, there are no HCP-type structures with more than 50% of all tetrahedral voids occupied. Here is a summary of various examples of HCP and CCP arrangements of X atoms stuffed with atoms in either octahedra $M^{(O)}$, tetrahedra $M^{(T)}$, or both simultaneously:

Fraction Octahedral Voids Filled by $M^{(O)}$	Fraction Tetrahedral Voids Filled by $M^{(T)}$	Close Packed Layer Sequence (X)		Chemical Formula	$\langle CN \rangle_X$
		HCP: ... <i>h</i> ...	CCP: ... <i>c</i> ...		
---	1	---	Li ₂ O; CaF ₂	$M^{(T)}_2X$	8
---	3/4	---	Bi ₂ O ₃ ; Mn ₂ O ₃	$M^{(T)}_3X_2$	6
---	1/2	ZnO; β-BeO	ZnS; PtS; PbO	$M^{(T)}X$	4
---	1/3	α-Ga ₂ S ₃	γ-Ga ₂ S ₃	$M^{(T)}_2X_3$	2.67 (2×3; 1×2)
---	1/4	γ-ZnCl ₂	SiS ₂ ; HgI ₂ ; Cu ₂ O	$M^{(T)}X_2$	2

---	1/6	Al ₂ Cl ₆	In ₂ I ₆	M ^(T) X ₃	1.33 (2× 1; 1× 2)
---	1/8	SnBr ₄	SnI ₄	M ^(T) X ₄	1
Fraction Octahedral Voids Filled by M ^(O)	Fraction Tetrahedral Voids Filled by M ^(T)	Close Packed Layer Sequence (X)		Chemical Formula	⟨CN⟩ _x
		HCP: ...h...	CCP: ...c...		
1	---	NiAs	NaCl	M ^(O) X	6
2/3	---	α-Al ₂ O ₃	---	M ^(O) ₂ X ₃	4
1/2	---	CaCl ₂ ; Rutile; CdI ₂	Anatase; CdCl ₂	M ^(O) X ₂	3
1/3	---	ZrI ₃ ; BiI ₃	YCl ₃	M ^(O) X ₃	2
1/4	---	α-NbI ₄ ; IrF ₄	NbF ₄	M ^(O) X ₄	1.5 (2× 2; 2× 1)
1/5	---	Nb ₂ Cl ₁₀ ; Ru ₄ F ₂₀	U ₂ Cl ₁₀ ; Mo ₄ F ₂₀	M ^(O) X ₅	1.2 (1× 2; 4× 1)
1/6	---	α-WCl ₆	---	M ^(O) X ₆	1
1	1	Na ₃ As*	Li ₃ Bi; α-BiF ₃	M ^(T) ₂ M ^(O) X	8 M ^(T) + 6 M ^(O)
1/8	1/2	---	Co ₉ S ₈	M ^(T) ₈ M ^(O) X ₈	4.75 (6× 5; 2× 4)
1/2	1/8	Mg ₂ SiO ₄	MgAl ₂ O ₄	M ^(T) M ^(O) ₂ X ₄	4
1/2	1/6	---	β-Ga ₂ S ₃	M ^(T) M ^(O) X ₃	3.33 (1× 4; 2× 3)
1/4	1/8	CrPS ₄	CrVO ₄	M ^(T) M ^(O) X ₄	2.5 (2× 3; 2× 2)

* G. Brauer, E. Zintl, *Z. Phys. Chem. B* **1937**, 37, 323-352. As atoms are not ideally HCP packed: $c/a = 1.77$. At high pressures, it is hexagonal LaF₃-type, with distorted HCP-packed As atoms but octahedral holes are empty. Nevertheless, $c/a \sim 1.77$ in the high-pressure structures.⁴⁵

To ensure that every close packed atom X is bonded to at least one other atom, $\frac{1}{8}$ of all tetrahedral or $\frac{1}{6}$ of all octahedral voids must be occupied. Furthermore, molecular solid-state structures arise when either tetrahedral or octahedral voids are less than $\frac{1}{4}$ filled. Filling all tetrahedral M^(T) and octahedral M^(O) voids in eutactic arrays of X atoms leads to M^(T)₂M^(O)X, or M₃X if there is no difference between M^(T) and M^(O). Only one example (Na₃As) occurs for HCP structures, but the c/a ratio is significantly larger (1.77) than the ideal value (1.633) because there are occupied face-sharing tetrahedra. On the other hand, there are numerous cubic Li₃Bi-type examples for CCP structures.

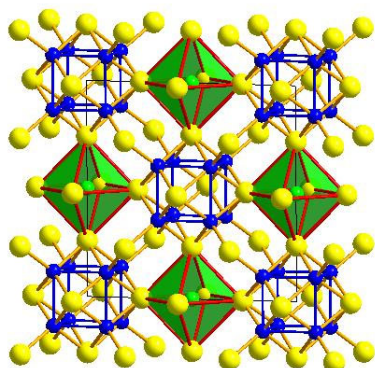
Other families of structures with combined tetrahedral and octahedral hole occupancies that occur in Nature include the pentlandites (Co₉S₈-type), olivines (Mg₂SiO₄-type) and spinels (MgAl₂O₄-type). Pentlandite, specifically Co₉S₈,⁴⁶ belongs to a class of sulfide minerals that are sources of Fe, Co, and Ni, in which $\frac{1}{2}$ of tetrahedral holes and $\frac{1}{8}$ of octahedral holes are occupied by 3d metal atoms. The arrangement of occupied tetrahedral holes forms Co₈ cubes with each face capped by one S atom; the octahedrally coordinated Co atom links six [Co₈S₆] clusters together. Pentlandites exist over a narrow range of total valence electron count close to 129e⁻ per T₉S₈ formula unit (T = some mixture of Fe, Co, Ni). Spinel, like MgAl₂O₄,⁴⁷ and olivines, such as

⁴⁵ H.J. Beister, K Syassen, J Klein, *Z. Naturforsch. B* **1990**, 45, 1388-1392; P. Hafner, KJ Range, *J. Alloys Cmpds*, **1994**, 216, 7-10.

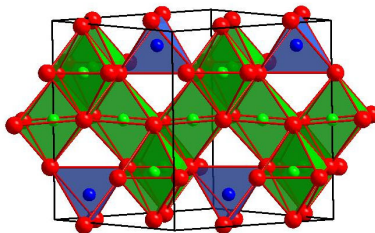
⁴⁶ S. Geller, *Acta Crystallogr.* **1962**, 15, 1195-1198.

⁴⁷ G.E. Bacon, *Acta. Crystallogr.* **1952**, 5, 684-686.

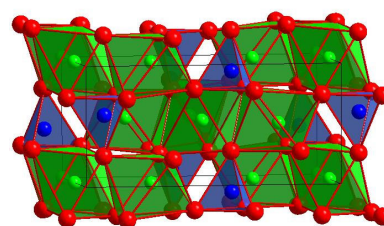
Mg_2SiO_4 ,⁴⁸ are based, respectively, on CCP and HCP oxide ions. In both structures, $\frac{1}{2}$ of octahedral holes and $\frac{1}{8}$ of tetrahedral holes are occupied. In MgAl_2O_4 , divalent Mg occupy tetrahedra and trivalent Al occupy octahedra, which are *normal spinels* because all divalent cations occupy tetrahedra and all trivalent cations occupy octahedra. Examples like CoFe_2O_4 , which is formulated as $\text{Co}^{2+}(\text{Fe}^{3+})_2(\text{O}^{2-})_4$, are *inverse spinels* because one-half the trivalent Fe^{3+} ions occupy the tetrahedra, whereas the divalent Co^{2+} and one-half the trivalent Fe^{3+} ions occupy the octahedra. Olivine is a solid solution between forsterite, Mg_2SiO_4 , and fayalite, Fe_2SiO_4 , and crystallizes in an orthorhombic crystal class, space group *Pbnm* with separated $[\text{SiO}_4]$ tetrahedra.



Pentlandite (*cF68*)
CoCo₈S₈



Spinel (*cF56*)
MgAl₂O₄



Olivine (*oP28*)
Mg₂SiO₄

The last column in the table indicates the *average coordination number* $\langle \text{CN} \rangle_X$ of each close packed atom X by the M atoms in octahedral and tetrahedral holes. X atoms are often nonmetals or anions, and M atoms are metals or cations. For any structure with the formula M_mX_x , $\langle \text{CN} \rangle_X$ is determined by treating the structure as a network of atoms and M–X bonds. There is an average $\langle \text{CN} \rangle_X$ of M–X contacts at X atoms; likewise, there is an average $\langle \text{CN} \rangle_M$ of M–X contacts at M atoms. Therefore, the relationship between $\langle \text{CN} \rangle_X$ and $\langle \text{CN} \rangle_M$ is

$$m \cdot \langle \text{CN} \rangle_M = x \cdot \langle \text{CN} \rangle_X.$$

This equation is just another expression of the “Rule of Stoichiometry” of the Bond-Valence Method that the total coordination at M atoms equals the total coordination at X atoms. For these eutactic structures, the equation becomes

$$6m = x \cdot \langle \text{CN} \rangle_X, \text{ for M occupying only octahedral voids} = \text{M}^{(\text{O})}, \text{ and}$$

$$4m = x \cdot \langle \text{CN} \rangle_X, \text{ for M occupying only tetrahedral voids} = \text{M}^{(\text{T})}.$$

According to the table, some $\langle \text{CN} \rangle_X$ values are not integers. For these cases, there must be more than one type of X atom in the structure. For example, consider $\text{M}^{(\text{T})}_2\text{X}_3$ like α - or γ - Ga_2S_3 , with M (Ga) atoms occupying only tetrahedral holes. Then, $m = 2$, $x = 3$, and using the second equation

$$4 \cdot 2 = 3 \cdot \langle \text{CN} \rangle_S, \text{ or } \langle \text{CN} \rangle_S = 2.67.$$

A reasonable solution is 2 S atoms (66.7%) coordinated by 3 Ga atoms and 1 S atom (33.3%) coordinated by 2 Ga atoms, which does match the observed crystal structure.⁴⁹ However, another possible solution is 2 S atoms (66.7%) coordinated by 2 Ga atoms and 1 S atom (33.3%) coordinated by 4 Ga atoms.

⁴⁸ J.D. Birlle, G.V. Gibbs, P.B. Moore, J.V. Smith, *Amer. Miner.* **1968**, 53, 807-824.

⁴⁹ G. Collin, J. Flahaut, M. Guittard, A. Loireau-Lozach, *Mater. Res. Bull.* **1976**, 11, 285-292.

If both octahedral and tetrahedral holes are occupied by M atoms so that the chemical formula is $M^{(T)}_m M^{(O)}_n X_x$, then the “Rule of Stoichiometry” becomes

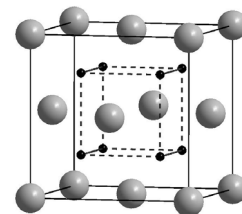
$$4m + 6n = x \cdot \langle \text{CN} \rangle_X.$$

As an example, consider $\text{Co}_9\text{S}_8 = \text{Co}^{(T)}_8\text{Co}^{(O)}\text{S}_8$. Then, $m = 8$, $n = 1$, $x = 8$, and the average coordination number of S by Co is $4.75 = (4 \cdot 8 + 6 \cdot 1) / 8 = 38 / 8$. In the crystal structure of Co_9S_8 , 6 S atoms (75%) are 5-coordinate, and 2 S atoms (25%) are 4-coordinate by Co atoms.

Pauling’s fifth rule, “*the number of essentially different kinds of constituent in a crystal tends to be small,*” suggests that stable structures should be inherently simple with elements of a given kind existing in as few different environments within a solid as possible. Eutactic structures tend to follow this qualitative “rule”. In the following few slides, we will examine certain important eutactic structures and address some simple chemical rationales for their stability.

(42) Eutactic Structures with Occupied Tetrahedral Voids: If tetrahedral holes in eutactic arrays of X atoms are occupied so that every X atom is coordinated to at least one $M^{(T)}$ atom, then chemical compositions can range from $M^{(T)}X_4$, with $1/8$ of all tetrahedral holes occupied and $\langle \text{CN} \rangle_X = 1$, to $M^{(T)}_2X$, with all tetrahedral holes occupied and $\langle \text{CN} \rangle_X = 8$.

100% Occupied Tetrahedral Voids: Filling all tetrahedral holes is only observed for CCP ($cF12$), as seen for the cubic structures of CaF_2 (fluorite) and Li_2O (“anti-fluorite”). In one CCP unit cell with space group $Fm\bar{3}m$, the eutactic array of X atoms occupy the Wyckoff $4a$ sites $(0, 0, 0)$, etc., and centers of the tetrahedral voids are located at the Wyckoff $8c$ sites $(1/4, 1/4, 1/4)$, etc. These 8 positions form a cube within the unit cell (see figure). In CaF_2 , calcium ions form the CCP array with F atoms occupying the tetrahedral holes and forming a cube around each Ca atom. In Li_2O , oxide ions form the CCP array and Li ions occupy the tetrahedral holes. Each $[\text{LiO}_4]$ or $[\text{FCa}_4]$ tetrahedron shares all six of its edges with neighboring tetrahedra. This structure type is adopted by many lanthanide dihydrides such as LaH_2 and LuH_2 , tetravalent oxides like ZrO_2 , and alkali metal chalcogenides such as Na_2S and K_2Se .



Filling all tetrahedral voids of HCP arrays results in a structure with space group $P6_3/mmc$. The eutactic arrangement of X atoms occupy Wyckoff $2d$ sites $(2/3, 1/3, 1/4)$, etc. and tetrahedral centers $M^{(T)}$ occur at Wyckoff $4e$ sites $(1/3, 2/3, z \sim 3/8)$. Because tetrahedra of X atoms share faces along the c -direction, the resulting $M^{(T)}-M^{(T)}$ distance would be too small to accommodate simultaneous occupation of these voids by any atoms. Therefore, no examples are known. In fact, to avoid simultaneous occupation of two adjacent $M^{(T)}$ sites, the maximum occupation of tetrahedral holes in an HCP array is 50%.

(43) 50% Occupied Tetrahedral Voids: The wurtzite (ZnO) structure ($hP4$), with space group $P6_3mc$, is the result for an HCP array of O atoms with Zn atoms in tetrahedral voids. The sphalerite or zinc blende (ZnS) structure ($cF8$), with space group $F4\bar{3}m$, is the corresponding solution for CCP eutactic arrays. In fact, if both sets of atoms $M^{(T)}$ and X are identical in the sphalerite structure, then the cubic diamond-type structure results. In both structures, each atom type (Zn and S or O) is coordinated by tetrahedra, all of which share vertices to form the 3-d extended structures. Furthermore, both structure types are noncentrosymmetric, i.e., neither one has inversion symmetry. In addition, the space group for wurtzite is polar because there is no unique origin. These structure types form for binary octet compounds such as trivalent pnictides (GaAs) and divalent chalcogenides (CdTe). Some compounds may form in each structure type, a

phenomenon called *polymorphism*. The illustrations also reveal that both structure types involve bonding networks of 6-membered rings as seen in cyclohexane, which exist in both “chair” and “boat” conformations. All 6-rings in sphalerite are “chair”, whereas “boat”-shaped 6-rings link layers of “chair”-shaped 6-rings in wurtzite along the *c*-direction.

(44) When fractions of void sites in a eutactic packing are occupied, different filling patterns and, therefore, structures are possible arising from various short-range and long-range structural driving forces, such as (short-range) covalent bonding and (longer-range) electrostatic interactions (“ionic bonds”). Therefore, many structures represent compromises among various interatomic forces. Nevertheless, the observed structure for any given chemical composition must be a minimum on a potential energy surface. These assertions are evident by examining three possible structures derived from occupying 50% of all tetrahedral voids in CCP arrays of X atoms: ZnS; PtS; and PbO structure types. Because each compound has 1:1 molar composition, the coordination of each X atom in the CCP array is 4-coordinate, but the specific geometry depends on the pattern of occupied tetrahedral voids.

- (a) ZnS (*cF8*; $F\bar{4}3m$, $a = 5.409 \text{ \AA}$; S at $4a$, Zn at $4c$): Within one unit cell of CCP S atoms, the four tetrahedral voids occupied by Zn atoms are located on alternating vertices of the dashed “cube” (see figure in the notes for (42)). This pattern provides maximum separation among all occupied tetrahedral voids as well as establishes tetrahedral coordination at S atoms by Zn atoms. By formulating ZnS as $\text{Zn}^{2+}\text{S}^{2-}$, both components are closed shell species: Zn^{2+} is $[\text{Ar}]3d^{10}$ and S^{2-} is $[\text{Ne}]3s^23p^6$. According to VSEPR, the four electron pairs at each sulfide site favor tetrahedral coordination. Through a combination of ligand field theory and the relative sizes of Zn^{2+} and S^{2-} (ratio of ionic radii is ~ 0.40), tetrahedral coordination at Zn sites is also preferred. Therefore, the structure of cubic ZnS (sphalerite) optimizes short-range polar-covalent Zn–S interactions and minimizes longer range ionic repulsions under the constraint of a 4-bonded network of atoms.
- (b) PtS (*tP4*; $P4_2/mmc$, $a = 3.47 \text{ \AA}$, $c = 6.11 \text{ \AA}$; Pt at $2c$, S at $2e$): Pt atoms form the eutactic CCP array and S atoms occupy four tetrahedral voids on two opposite edges of the “cube” (again, see figure in the notes for (42)). Upon relaxation, which extends the CCP array along a single direction (*c*-axis), this occupation pattern creates the tetragonal structure of PtS with a single Pt–S distance (2.31 \AA).⁵⁰ In this structure of PtS, Pt atoms are nearly square planar coordinated by S, with S–Pt–S angles of 82.7° and 97.3° rather than 90° . Likewise, the $[\text{SPt}_4]$ tetrahedra are distorted having angles $97.3^\circ(2\times)$ and $115.9^\circ(4\times)$. According to the formulation $\text{Pt}^{2+}\text{S}^{2-}$, ligand field theory rationalizes a square planar environment for a 16-electron, $5d^8$ ion like Pt^{2+} , and VSEPR accounts for tetrahedral coordination at the octet ion S^{2-} . Using the constraint of a single, fixed Pt–S distance, the maximum volume structure minimizes longer range ionic repulsions between pairs of cations and pairs of anions, creating idealized tetrahedral coordination around S atoms and giving $c/a = \sqrt{2} = 1.41$ for the tetragonal cell. On the other hand, if the coordination at Pt would be ideally square planar to optimize Pt–S covalent bonding, then $c/a = 2$. Since the measured unit cell ratio $c/a = 1.76$, the observed structure of PtS represents a *compromise* between optimizing ionic and covalent bonding forces.⁴⁴
- (c) PbO (*tP4*; $P4/nmm$, $a = 3.947 \text{ \AA}$, $c = 4.988 \text{ \AA}$; Pb at $2c$ ($z = 0.239$), O at $2a$): Pb atoms form a CCP eutactic array and O atoms occupy tetrahedra on one face of the “cube” (again, see

⁵⁰ A. Kjekshus, *Acta Chem. Scand.* **1966**, 20, 577-579.

figure in the notes for (42)) to create the layered structure of red-PbO (litharge).⁵¹ The O atoms form planar square nets and the Pb atoms sit alternately above and below adjacent squares giving [PbO] layers with Pb atoms in square pyramidal coordination to O atoms. From the formulation $\text{Pb}^{2+}\text{O}^{2-}$, the electronic configuration of Pb^{2+} is $[\text{Xe}4f^{14}5d^{10}]6s^2$ and the asymmetric 4-coordination at Pb suggests the lone pair to be stereochemically active. $\text{Pb}\cdots\text{Pb}$ interactions arising from some $6s$ - $6p$ hybridization contribute to holding the [PbO] layers together.⁵² From a different perspective, an ideal CCP array of Pb atoms would give $c/a = \sqrt{2} = 1.41$ for the unit cell of PbO. However, the CCP array of Pb atoms is compressed along the c -direction, yielding the experimental $c/a = 1.26$. Compression of the CCP unit cell along c can lead to BCC packing when $c/a = 1.00$. Therefore, the structure of red-PbO represents a compromise between FCC and BCC atomic packings of Pb^{2+} sites. These layers are also found in the iron chalcogenide superconductors related to FeSe.

(45) Eutactic Structures with Occupied Octahedral Voids: If octahedral holes in eutactic arrays of X atoms are occupied so that every X atom is coordinated to at least one $\text{M}^{(O)}$ atom, then chemical compositions can range from $\text{M}^{(O)}\text{X}_6$, with $\frac{1}{6}$ of all octahedral holes occupied and $\langle \text{CN} \rangle_{\text{X}} = 1$, to $\text{M}^{(O)}\text{X}$, with all octahedral holes occupied and $\langle \text{CN} \rangle_{\text{X}} = 6$.

100% Occupied Octahedral Voids: Filling all octahedral voids gives the two limiting cases: cubic NaCl-type for CCP and hexagonal NiAs-type for HCP arrays. In NaCl with space group $Fm\bar{3}m$, each Cl atom of the CCP eutactic array is octahedrally coordinated by Na atoms, which fill the octahedral holes. The $[\text{NaCl}_6]$ octahedra share edges and vertices, so there are no exceedingly short Na–Na contacts. This structure occurs for numerous binary octet compounds, such as monovalent metal halides (NaCl, AgBr), divalent metal oxides and heavier chalcogenides (BaSe), and trivalent metal pnictides (LaBi). Among NaCl-type transition metal monoxides, like “FeO” and “CoO”, there are often vacancies or substitutional and interstitial defects. In hexagonal NiAs, As atoms form an HCP eutactic array. The octahedral voids, completely occupied by Ni atoms, share faces along the c -axis. As a result, the sixfold coordination at As by Ni atoms is trigonal prismatic and there are short Ni–Ni distances along the c -axis. Therefore, NiAs-type structures occur for transition metal compounds that allow metal-metal bonding, e.g., transition metal pnictides and chalcogenides with metal d -electron configurations ranging from d^1 in TiSb to d^8 in NiTe. Since the structural influence of metal-metal bonding can depend on the net valence electron count of the transition metals, binary NiAs-type compounds show a wide range of c/a ratios, as listed in the table below:

X in TX	Group #:	4	5	6	7	8	9	10
As		Ti: 1.68		Cr: 1.60	Mn: 1.53		Co: 1.46	Ni: 1.39
Sb		Ti: 1.55	V: 1.28 Nb: 1.28	Cr: 1.33	Mn: 1.39	Fe: 1.26	Co: 1.34	Ni: 1.30 Pd: 1.38
Bi					Mn: 1.43		Rh: 1.39	Ni: 1.31 Pd: 1.35
S		Ti: 1.94	V: 1.73 Nb: 1.95	Cr: 1.55		Fe: 1.69	Co: 1.53	Ni: 1.55
Se				Cr: 1.64	Mn: 1.63	Fe: 1.62	Co: 1.47 Rh: 1.51	Ni: 1.46

⁵¹ W.J. Moore, L. Pauling, *J. Am. Chem. Soc.* **1941**, 63, 1392-1394.

⁵² G. Trinquier, R. Hoffmann, *J. Phys. Chem.* **1984**, 88, 6696-6711.

Te	Ti: 1.67	V: 1.54	Cr: 1.56	Mn: 1.62	Fe: 1.49	Co: 1.38	Ni: 1.35
	Zr: 1.68					Rh: 1.42	Pd: 1.38

Most of these structures have c/a ratios less than the ideal value (1.63) for HCP arrays of X atoms, especially for high d -electron configurations. Compounds like “ScS” and CdTe with nearly empty or filled valence d subshells do not allow sufficient metal-metal bonding to stabilize the NiAs-type structure. As a result, they adopt halite (NaCl) or sphalerite (ZnS) structure types.

(46) 50% Occupied Octahedral Voids: An important set of structures occurs for eutactic arrays with $\frac{1}{2}$ of all octahedral voids occupied. As seen for partial occupation of tetrahedral holes, there are numerous patterns possible for occupying octahedral voids. Layered structures arise when planes of octahedra are occupied alternately 100% and 0% along the stacking direction of the eutactic array. Rhombohedral CdCl₂ is the representative for CCP, and hexagonal CdI₂ is the representative for HCP. In both structure types, the close packed atoms (Cl or I) are three-coordinate, each forming a [ClCd₃] or [ICd₃] trigonal pyramid. In CdI₂ itself, the c/a ratio is 1.616, which is slightly lower than the ideal HCP value of 1.633. The [M^(O)X₂] layers are held together by van der Waals interactions, so such compounds often exist in different polymorphs based upon various stacking arrangements of the layers. In general, the HCP-based CdI₂-type is observed for softer Lewis bases like chalcogenides, bromides, and iodides, whereas the CCP-based CdCl₂ is found for harder Lewis bases like chlorides; the anti-CdCl₂-type also exists for di-metal carbides such as rare-earth carbides.

Another occupation pattern is for each layer of octahedral holes to be 50% occupied along the stacking direction of the eutactic array. For CCP, the result is the tetragonal anatase-type structure of TiO₂; for HCP, it is the orthorhombic structure of CaCl₂. In HCP-based CaCl₂, the pattern of filling octahedral voids destroys the hexagonal symmetry of the empty eutactic packing and becomes orthorhombic. The local coordination at the Cl atom sites is trigonal pyramidal [ClCa₃], but it is closer to trigonal planar than for the anions in the hexagonal CdI₂-type. A slight distortion of CaCl₂ by puckering the 2-d eutactic planes of Cl atoms²² leads to the tetragonal rutile-type structure observed for TiO₂ and numerous metal dioxides and difluorides. The puckering creates nearly trigonal planar coordination about the close packed atoms, such as [OTi₃] in rutile TiO₂. Although minimizing the electrostatic Madelung energy can be one driving force, effective π -overlap between filled $2p$ orbitals on O atoms with empty $3d$ orbitals on Ti atoms may also influence the planar coordination at O atoms.⁵³ The analogue based upon the CCP array gives the anatase structure of TiO₂. If the CCP array of oxide ions would remain undistorted after $\frac{1}{2}$ of the octahedral voids are occupied by Ti atoms, each O atom would have a planar T-shaped [OTi₃] coordination, which does not optimize Ti–O polar-covalent bonding.⁵³ As a result, the T-shaped [OTi₃] units distort toward trigonal planar, but the atomic shifts severely distort each [TiO₆] octahedron. Therefore, the tetragonal anatase structure of TiO₂ represents a compromise of keeping nearly regular [TiO₆] octahedra and allowing trigonal planar [OTi₃] units. Anatase is the “kinetically stable” form of TiO₂ found in reagent bottles of “TiO₂”. Upon heating anatase to approximately 1000°C, it irreversibly transforms into the rutile form.

⁵³ J.K. Burdett, T. Hughbanks, G.J. Miller, J.W. Richardson, Jr., J.V. Smith, *Inorg. Chem.* **1985**, 24, 2244-2253.

The following table, reproduced from Wells, lists the structures of 3d metal dihalides:

MX_2	Mg	Ti	V	Cr	Mn	Fe	Co	Ni	Cu	Zn	
F	R		R	R*	R	R	R	R	R*	R	R = rutile; R* = distorted rutile
Cl	C	I	I	R*	C	C	C	C	I*	Tet	C = CdCl ₂
Br	I	I	I	I*	I	I	C/I	I	I*	Tet	I = CdI ₂ ; I* = distorted CdI ₂
I	I	I	I	I*	I	I	I	C		Tet	Tet = tetrahedral network

Other fractions and their patterns of partially filled tetrahedral or octahedral holes in eutactic packing arrays lead to numerous structures, producing *polymorphism* and *concentration waves*. As mentioned above, polymorphism arises when a compound adopts many different structural arrangements because the energy differences among these different forms is small, generally when compared to kT . One significant case is silicon carbide, which is a tetrahedral network of alternating Si and C atoms. The two simplest structures are the 3C sphalerite-type and 2H wurtzite-type *polytypes*. Numerous other hexagonal and rhombohedral stacking variants are possible, leading to over 250 polytypes.

Concentration waves are variations in the occupancy fractions of the tetrahedral or octahedral holes along the stacking direction. These “waves” in the structure can be periodic or aperiodic. Periodic concentration waves, as observed for various sulfides of titanium, chromium, and iron,⁵⁴ create large *superstructures* of the unit cell based upon eutactic arrays. A frequent example occurs in the sequence available between hexagonal CdI₂-type and NiAs-type structures, a series that fills between $\frac{1}{2}$ and all octahedral voids in a HCP eutactic array. One example is Rh_{1+x}Te₂ ($\sim 0.08 < x < 0.90$). At $x = 0.5$, i.e., Rh_{1.5}Te₂ = Rh₃Te₄, the structure is completely ordered. For other compositions, some octahedral voids are partially occupied, whereas some are completely filled. Throughout this system, the concentration wave alternates $\cdots 1 \cdots x \cdots 1 \cdots x \cdots$ along the stacking of close packed planes of octahedral voids. For $x < 0.5$, this pattern creates a fraction of Rh-Rh-Rh trimers along the stacking direction, so we can formulate Rh_{1+x}Te₂ as (Rh₃)_xRh_{1-2x}Te₂. At $x = \frac{1}{2}$, there are only Rh-Rh-Rh trimers. When $x > 0.5$, then there can exist Rh₃, Rh₇, Rh₁₁, etc. chains according to the pattern of how Rh atoms occupy the octahedral holes. There are electronic reasons for this pattern of structures as evaluated by electronic structure calculations.⁵⁵

(47) Iron Oxides: Three types of naturally occurring iron oxides form an important collection of structures based on eutectic arrays of oxide ions containing Fe²⁺ and Fe³⁺ in octahedral and tetrahedral voids:

Hematite ($\alpha\text{-Fe}_2\text{O}_3$) is found in many rocks and soils and occurs in colors ranging from black to brown to red. It is electrically conductive with a crystal structure based upon an HCP array of oxide ions with $\frac{2}{3}$ octahedral holes occupied by Fe³⁺ ions, isotypic to corundum (Al₂O₃) with space group $R\bar{3}c$ and Pearson symbol $hR30$. Every plane of octahedral holes is equally occupied. As a result of the occupation pattern in the HCP oxide array, there are pairs of Fe³⁺ ions in octahedra sharing faces along c . However, the metal atoms shift off-center and away from each other giving a long Fe \cdots Fe distance of ~ 2.88 Å. Although this distance is rather long for Fe–Fe bonding, through-space (direct) and through-bond (indirect) magnetic exchange interactions are possible. $\alpha\text{-Fe}_2\text{O}_3$ is an antiferromagnet with moments parallel to c at temperatures below 250

⁵⁴ F. Jellinek, *Int. Rev. Sci.: Inorg. Chem., Ser. 1* **1972**, 5, 339-396.

⁵⁵ C.-S. Lee, G.J. Miller, *Inorg. Chem.* **1999**, 38, 5139-5150.

K; above 250 K, the moments reorient perpendicular to c , showing canted antiferromagnetic coupling or weak ferromagnetism until the Néel temperature of 948 K; above 948 K, hematite is paramagnetic.

Magnetite (Fe_3O_4) is a black, metallic, and ferromagnetic mineral. It adopts the spinel-type structure, space group $Fd\bar{3}m$ and Pearson symbol $cF56$, which involves a CCP array of oxide ions and $\frac{1}{2}$ octahedral and $\frac{1}{8}$ tetrahedral holes occupied by iron ions. It is considered to be an *inverse spinel* with Fe^{3+} ions occupying the tetrahedra and equal amounts of Fe^{3+} and Fe^{2+} ions occupying the octahedra to give the formulation: $\text{Fe}^{2+}(\text{Fe}^{3+})_2\text{O}_4 = (\text{Fe}^{3+})_{\text{Tet}}(\text{Fe}^{2+}\text{Fe}^{3+})_{\text{Oct}}\text{O}_4$. However, given the metallic behavior, mixed valency is questionable. At ~ 120 K, magnetite undergoes the Verwey transition, which is a metal-to-insulator transition that includes a change in crystal symmetry from cubic to monoclinic. The Curie temperature is 853 K.

Wüstite⁵⁶ is a nonstoichiometric compound formulated simply as Fe_{1-x}O ($0.04 < x < 0.12$) that is found in meteorites and with native iron. “Ideal” wüstite, i.e., stoichiometric “FeO” in the halite structure, is not stable at pressures below 10 GPa (98,700 atm). A more representative formula indicates mixed valent iron: $(\text{Fe}^{3+})_{1-3x}(\text{Fe}^{2+})_{2x}\text{O}$. X-ray diffraction and Mössbauer spectroscopic studies reveal that ferric ions can occupy both octahedral and tetrahedral voids of the CCP array of oxide ions. Electrical conductivity and magnetic properties of Fe_{1-x}O are sensitive to the degree of nonstoichiometry and the distribution of vacancies and interstitial defects of the halite-type framework.

Vacancies: In crystalline structures, defects such as vacant atomic sites and interstitial atoms can have profound effects on physical properties. They can naturally arise from entropic influences, so that the concentrations of vacancies and interstitials in a crystalline solid are typically quite low and not easily accessible by many experimental techniques like refinements from X-ray diffraction patterns. However, there can also be enthalpic reasons for these types of crystalline defects, especially the formation and pattern of vacancies in a structure. As seen in the iron oxide wüstite, vacancy concentration at the iron sites influences oxidation states. At low levels of iron vacancies, their distribution is random. At larger levels, ordered arrangements occur as in magnetite and hematite. From the perspective of structural chemistry, vacancy patterns in crystalline structures can be driven by anion coordination environments controlled by lone pairs and cation clusters induced by metal-metal bonding.

(48) Scandium Monosulfide: ScS is a d^1 compound adopting the cubic NaCl-type structure,⁵⁷ but it is not a *line compound*. Rather, ScS is one composition within a continuous Sc:S molar ratio varying from ~ 0.80 ($\text{Sc}_{0.80}\text{S} = \text{ScS}_{1.25}$) to 1.15 ($\text{Sc}_{1.15}\text{S} = \text{ScS}_{0.87}$). Therefore, “ScS” is one member of a *homogeneity range* that is formulated as $\text{Sc}_{1\pm x}\text{S}$. Every member $\text{Sc}_{1\pm x}\text{S}$ shows an X-ray diffraction pattern consistent with the cubic halite structure (space group $Fm\bar{3}m$ with S atoms at $4a$ sites and Sc atoms at $4b$ sites), and gives a maximum lattice constant and cell volume close to the ideal composition “ScS”. The nonstoichiometric compositions $\text{Sc}_{1\pm x}\text{S}$ require either vacancies or atoms in interstitial positions. Since experiments conclude the absence of interstitials, the parent halite structure must contain vacant sites on the S sites for Sc-rich Sc_{1+x}S or the Sc sites for S-rich Sc_{1-x}S . The diffraction results, at the level of resolution reported, also suggest the vacancies to be randomly arranged throughout the bulk structure.

⁵⁶ R.M. Hazen, R. Jeanloz, *Rev. Geophys. Space Phys.* **1984**, 22, 37-46.

⁵⁷ J.P. Dismukes, J.G. White, *Inorg. Chem.* **1964**, 3, 1220-1228.

Possible clues about the structural chemistry of the S-rich NaCl-type phase region Sc_{1-x}S may be ascertained from the orthorhombic structure of Sc_2S_3 (space group $Fddd$, $oF80$; $a = 10.41 \text{ \AA}$, $b = 7.38 \text{ \AA}$, $c = 22.05 \text{ \AA}$). It consists of a CCP array of sulfide ions with $\frac{2}{3}$ octahedral holes occupied by Sc^{3+} ions to give an ordered vacancy superstructure of the NaCl-structure type. The orthorhombic lattice vectors of Sc_2S_3 are related to specific directions of the NaCl-type as follows:

$$a \sim 2a_{\text{NaCl}} ([002]); b \sim \sqrt{2}a_{\text{NaCl}} ([1\bar{1}0]); \text{ and } c \sim 3\sqrt{2}a_{\text{NaCl}} ([330]).$$

Every S atom in Sc_2S_3 is coordinated by 4 Sc atoms in a manner that resembles SF_4 , i.e., a *cis*-divacant octahedral (“sawhorse”) environment. Therefore, for the S-rich region Sc_{1-x}S , vacancies at the Sc positions likely occur to create the “sawhorse” coordination environment at some S atoms.⁵⁸ To accomplish this, though, there must also be 5-coordinate, square pyramidal arrangements at other S atoms.

For the Sc-rich region Sc_{1+x}S , vacancies at the S positions create empty metal octahedra (“ Sc_6 ”). For low concentrations of vacancies, there is a high probability that the nearby S atom positions are occupied. Therefore, surrounding each vacant S position is a $[\text{Sc}_6\text{S}_{12}]$ environment with the 12 S atoms bridging each edge of the Sc_6 octahedron. These types of metal clusters with edges bridged by anionic ligands, called “6-12 clusters”, are quite common for transition metals in groups 3-5, e.g., Y, Zr, and Nb.

Now, what does this discussion imply about the actual structure of scandium monosulfide ScS ? Because this compound is one composition inside a broad phase region of the binary Sc-S system, then ScS likely has vacancies at both Sc and S sites simultaneously. An extensive theoretical study was undertaken to provide some elucidation, but this structural problem remains open.⁵⁹

(49) Niobium Monoxide: Vacancies can indeed occur simultaneously at both anion and cation sites in the halite-type structure. NbO is an example in which the arrangement of these vacancies realize a periodic structure. By starting with a hypothetical NaCl-type “ NbO ”, in which one unit cell contains 4 O atoms (at corners and face-centers; a CCP array) and 4 Nb atoms (at center and edge-centers), 1 O atom (at corners) and 1 Nb atom (at center) are removed to create $\text{Nb}_3\text{O}_3 = \text{NbO}$. A view of NbO along any of the body-diagonals of the cubic unit cell reveals channels of vacancies. The local coordination of both Nb and O is square planar (Nb–O is 2.15 \AA), which is promoted by O atom’s preference for π -type orbital overlaps (as opposed to S, which prefers the 4-coordinate sawhorse environment). Also, there is a single Nb–Nb distance of 2.98 \AA , which is well within metal-metal bonding interactions for d^3 Nb(II). Therefore, another perspective of NbO involves a 3-d network of Nb_6 octahedral clusters sharing vertices in all six directions. The O atoms bridge every edge to create Nb_6O_{12} clusters, like those proposed for the Sc-rich sulfides Sc_{1+x}S . We can write a *structural formula* for NbO using the Nb_6O_{12} cluster formula by recognizing that each Nb atom is shared between *two* clusters while each O atom is shared among *four* clusters: $\text{Nb}_{6/2}\text{O}_{12/4} = \text{Nb}_3\text{O}_3 \rightarrow \text{NbO}$. A study of the electronic structure of NbO reveals that Nb–Nb bonding is optimized because all Nb–Nb bonding states are filled and Nb–Nb antibonding states are empty in the electronic density of states.⁶⁰

⁵⁸ G.L.W. Hart, A. Zunger, *Phys. Rev. Lett.*, **2001**, 87, 275508.

⁵⁹ J.K. Burdett, J.F. Mitchell, *Chem. Mater.* **1993**, 5, 1465-1473; J.K. Burdett, S.C. Sevov, O.N. Mryasov, *J. Phys. Chem.* **1995**, 99, 2696-2700; S.M. Peiris, M.T. Green, D.L. Heinz, J.K. Burdett, *Inorg. Chem.* **1996**, 35, 6933-6936.

⁶⁰ J.K. Burdett, T. Hughbanks, *J. Am. Chem. Soc.* **1984**, 106, 3101-3113.

Metal-Metal Bonding in transition metal compounds manifests as extended networks or clusters surrounded by anions. The occurrence of metal-metal bonding generally distorts ideal structure types, as seen by the compression of the c/a ratio in NiAs-type compounds. To accommodate metal-metal bonding, the transition metals exist in reduced oxidation states so that the metal has a nonzero valence d -electron count.

(50) Clusters: Octahedral metal clusters dominate the reduced metal chemistry of early 4d and 5d transition metals from groups 3-6. They occur in two types which differ by the number and configuration of ligands surrounding the octahedron:

M₆X₁₂-type clusters exist for several transition metal halide systems, especially for binary group 5 metal halides such as Ta₆Cl₁₅ and Nb₆Cl₁₄.^{61,62} There are two types of ligands at the metal atoms: (1) inner (*innen*, from German) X⁽ⁱ⁾ bridging the 12 edges of the M₆ octahedron; and (2) outer (*ausser*, from German) X^(a) that are directed away from the cluster center. A diverse structural chemistry emerges for these clusters because the outer ligands can bridge multiple M₆X⁽ⁱ⁾₁₂ clusters in solids. They occur for 14-16 valence electrons for metal-metal bonding, an outcome that is rationalized by molecular orbital theory. For example,

Ta₆Cl₁₅ = [Ta₆]¹⁵⁺(Cl⁻)₁₅, which has $(6 \cdot 5e^- - 15e^-) = 15e^-$ for Ta-Ta bonding, and

Nb₆Cl₁₄ = [Nb₆]¹⁴⁺(Cl⁻)₁₄, which has $(6 \cdot 5e^- - 14e^-) = 16e^-$ for Nb-Nb bonding.

M₆X₈-type clusters are more common for group 6 metals, but also exist for group 5 metals,^{61,62,63} such as Mo₆Cl₁₂, Nb₆I₁₁, and Chevrel phases such as PbMo₆S₈ and HoMo₆S₈. Again, there are two types of ligands: (1) inner (*innen*) X⁽ⁱ⁾ capping the 8 edges of the M₆ octahedron; and (2) outer (*ausser*) X^(a) directed away from the cluster center. For the Chevrel phases, sulfides serve as inner ligands to one cluster and outer ligands to another cluster to create a 3-d network.⁶⁴ These clusters have 19-24 valence electrons for metal-metal bonding:

Nb₆I₁₁ = [Nb₆]¹¹⁺(I⁻)₁₁, which has $(6 \cdot 5e^- - 11e^-) = 19e^-$ for Nb-Nb bonding;

PbMo₆S₈ = Pb²⁺[Mo₆]¹⁴⁺(S²⁻)₈, which has $(2e^- + 6 \cdot 6e^- - 16e^-) = 22e^-$ for Mo-Mo bonding;

Mo₆Cl₁₂ = [Mo₆]¹²⁺(Cl⁻)₁₂, which has $(6 \cdot 6e^- - 12e^-) = 24e^-$ for Mo-Mo bonding.

Chevrel phases have garnered exceptional interest because they showed reasonably high superconducting critical temperatures (~15 K) and upper critical fields (~50 Tesla at 4.2 K) at the time of their discovery in 1971.⁶⁵

The structural chemistry of these clusters expands dramatically by considering interstitial species, which are formally anionic, inside the metal octahedron.⁶⁶ Very few M₆X₈ clusters accept interstitial atoms, presumably due to strong anion-anion repulsions through the faces of the octahedron. Nevertheless, one example is Nb₆I₁₁H, which forms by reaction of Nb₆I₁₁ with hydrogen. On the other hand, M₆X₁₂ clusters, which are conceptually derived from the NaCl-structure, can take on a wide range of main group and transition metal interstitials, especially for groups 3 and 4 metals, e.g., Zr₆Cl₁₄C and Zr₆Cl₁₄Fe. The interstitial atom adds valence electrons to the cluster but disrupts direct metal-metal bonding.

⁶¹ C. Perrin, S. Cordier, F. Gulo, A. Perrin, *Ferroelectrics*, **2001**, 254, 83-90.

⁶² N. Prokopuk, D.F. Shriver, *Adv. Inorg. Chem.* **1998**, 46, 1-49.

⁶³ T. Saito, *Adv. Inorg. Chem.* **1997**, 44, 45-91.

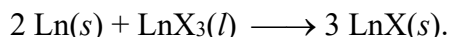
⁶⁴ O. Peña, *Physica C* **2015**, 514, 95-112.

⁶⁵ R. Chevrel, M. Sergent, J. Prigent, *J. Solid State Chem.* **1971**, 3, 515-519.

⁶⁶ D.G. Adolphson, J.D. Corbett, *Inorg. Chem.* **1976**, 15, 1820-1823.

(51) Condensed Clusters: The structural chemistry of octahedral clusters expands by condensing them via their edges and faces. An interesting class of structures is based upon the layered structure of ZrCl_2 ,⁶⁷ which consists of $[\text{ClZrZrCl}]$ slabs formed by two close-packed planes of Zr atoms sandwiched between two planes of Cl atoms. The Cl atoms cap opposite faces of octahedral holes, so that this structure can be described as a 2-d condensation of Zr_6Cl_8 clusters. Each Zr(II) ion uses its three valence $4d$ electrons for metal-metal bonding. Its crystal symmetry is rhombohedral, space group $R\bar{3}m$, and the unit cell contains three slabs. By projecting the atom positions on the ab -plane, the atoms and slabs stack along c as follows: $\cdots [\text{CABC}] [\text{ABCA}] [\text{BCAB}] \cdots$ (Cl atoms in *italics*; Zr atoms in **bold**).

Various lanthanide monohalides, such as “GdCl” and “TbBr”, were also reported to be isostructural with ZrCl_2 . These compounds were prepared by a *synproportionation* reaction of the metal powder $\text{Ln}(s)$ and molten lanthanide trihalide $\text{LnX}_3(l)$:

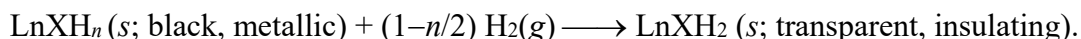


However, the yields of $\text{LnX}(s)$ were small and erratic because structural analysis by X-ray powder diffraction often gave somewhat different unit cell parameters for the same product. As it turned out, the reactants could be easily contaminated:

- The lanthanide trihalides were prepared by treating $\text{Ln}_2\text{O}_3(s)$ with $\text{NH}_4\text{X}(g)$, which generates $\text{NH}_3(g)$ and $\text{H}_2\text{O}(g)$ in addition to $\text{LnX}_3(s)$, but this procedure also yields the oxyhalide $\text{LnOX}(s)$. Nevertheless, $\text{LnX}_3(s)$ is conveniently separated from $\text{LnOX}(s)$ by sublimation.
- Lanthanide metal powders were obtained by hydrogen embrittlement. Metal chunks were treated with $\text{H}_2(g)$ to form metal hydrides, i.e., LnH_2 , LnH_{3-x} , or some mixture, which can be crushed into small particles and then dehydrogenated under vacuum, typically at a temperature $\sim 2/3$ melting point of the metal. This method is effective for lanthanides with high melting points, such as Gd, Tb, Dy, Ho, Tm and Lu, but is problematic for metals like Sm, Eu, and Yb, which have significant vapor pressures in the liquid state. Regardless, it is difficult to remove all H atoms from these lanthanide hydrides, so the starting metal powder $\text{Ln}(s)$ presumably contained significant amounts of interstitial H atoms.

After an intensive effort of synthesis and characterization, these so-called binary “lanthanide monohalides” were determined to be ternary lanthanide hydride halides, LnXH_n ($n = 0.66\text{--}1.00$). They could be obtained reproducibly and in high yields when controlled amounts of hydrogen or metal hydrides were used as reactants.

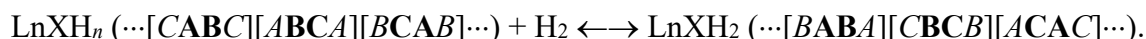
The compounds LnXH_n occur for many different lanthanide metals and the halogens Cl, Br, I.⁶⁸ H atoms occupy the tetrahedral holes between two adjacent close-packed Ln planes. Their structures resemble ZrCl_2 , but each slab is $[\text{Ln}_2\text{X}_2\text{H}_{2n}]$. At the highest H content LnXH , these formally d^1 compounds are black, metallic, and reflective powders. Under excess H_2 pressure and temperatures approaching 400°C , $\text{LnXH}_n(s)$ reacts with $\text{H}_2(g)$, becoming visibly transparent and electrically insulating, according to the reaction:



$\text{LnXH}_2(s)$ are formally d^0 compounds. In their structures, two H atoms occupy opposite faces of the octahedral holes while the tetrahedral holes remain occupied by H atoms. To avoid significant hydride-halide ion repulsions in LnXH_2 , planes of halide ions shift from capping the octahedra

⁶⁸ A. Simon, H.J. Mattausch, G.J. Miller, W. Bauhofer, R.K. Kremer, *Handbook of Physics and Chemistry of the Rare Earths*, Vol. 15, 1991, pp. 191-285.

faces to capping tetrahedra faces. Therefore, the change in hydride content causes a concerted movement of entire planes of halide atoms accordingly:



This concerted shift of atoms is an outcome of a *topotactic* reaction. When $\text{LnXH}_2(s)$ are treated with a moderate vacuum (ca. 10^{-4} atm) and temperatures of ca. 400-500° C, hydrogen gas is released to form the metallic hydride halide $\text{LnXH}_n(s)$.

(52) If transition metals are octahedrally coordinated, then metal-metal bonding enables formation of low-symmetry structures by distorting the octahedral ligand field to create a network of metal-metal bonds bridged by metal-ligand bonds. In an octahedral ligand field, the valence d orbitals are split into three t_{2g} orbitals with lobes directed between the ligands and two e_g orbitals with lobes directed toward the ligands. Therefore, metal-metal bonding utilizes the t_{2g} orbitals. As long as these orbitals are partially occupied, i.e., for d^1 - d^5 configurations, then metal-metal bonds can occur between either shared octahedral faces, as in NiAs-types, or shared octahedral edges, as in the CdI_2 - and rutile-types, the second of which are discussed here:

CdI_2 -Type: ZrTe_2 is hexagonal, space group $P\bar{3}m1$, with no short Te-Te contacts. Zr(IV) is d^0 and forms planar nets of equilateral triangles bridged by Te atoms. With no valence electrons for metal-metal bonding, the Zr-Zr distances (3.95 Å) are controlled by the Zr-Te bonds (2.90 Å). On the other hand, the planar nets of metals in NbTe_2 and MoTe_2 are distorted into ribbons due to metal-metal bonding. NbTe_2 is monoclinic, space group $C2/m$. Nb(IV) is d^1 and forms 3-stranded ribbons of Nb atoms along $b = 3.62$ Å. Shorter Nb-Nb distances (3.32 Å) between each strand lead to significantly distorted octahedral coordination for the Nb atoms at the edges of the ribbons. MoTe_2 is also monoclinic, space group $P2_1/m$. Mo(IV) is d^2 and forms 2-stranded ribbons, i.e., zig-zag chains, along $b = 3.47$ Å. Short Mo-Mo distances (2.89 Å) within the zig-zag chains distort the octahedral coordination at each Mo atom.

Rutile-Type: The pattern of half-occupied octahedral holes in an HCP array leads to this tetragonal structure with chains of *trans*-edge sharing octahedra and equal metal-metal distances along c . Examples among metal dioxides include insulating TiO_2 , VO_2 above $\sim 65^\circ\text{C}$, ferromagnetic CrO_2 , and RuO_2 . On the other hand, d^1 VO_2 below $\sim 65^\circ\text{C}$ and d^2 MoO_2 are monoclinic, space group $P2_1/c$, with alternating short-long metal-metal distances along the chains of edge-sharing octahedra. According to electronic structure calculations, the tetragonal structure for d^0 TiO_2 , high-spin d^2 CrO_2 , and d^4 RuO_2 occurs because these electron configurations do not promote metal-metal bonding.⁶⁹ Rutile-type d^1 VO_2 is metallic above $\sim 65^\circ\text{C}$ with equal V-V distances (2.87 Å) along c , but becomes semiconducting below $\sim 65^\circ\text{C}$ as the structure distorts to monoclinic with V-V distances alternating 2.61 Å and 3.18 Å.⁷⁰

(53) Ligand Effects from Metal-Metal Bonding: As pointed out for NbTe_2 , MoTe_2 , VO_2 , and MoO_2 , the formation of metal-metal bonds across octahedral edges distorts the ligand field. This effect is especially visible by microscopy in the layered group 5 halides Nb_3X_8 ⁷¹ and chalcogenide

⁶⁹ J.K. Burdett, *Acta Cryst.* **1995**, *B51*, 547-558.

⁷⁰ H. Lu, S. Clark, Y. Guo, J. Robertson, *J. Appl. Phys.* **2021**, *129*, 240902; F.J. Morin, *Phys. Rev. Lett.* **1959**, *3*, 34-36; A. Magnéli, G. Anderson, *Acta Chem. Scand.* **1955**, *9*, 1378-1381; J.M. Longo, P. Kierkegaard, *Acta Chem. Scand.* **1970**, *24*, 420-426.

⁷¹ A. Simon, H.G. von Schnering, *J. Less-Common Met.* **1966**, *11*, 31-46.

halides M_3YX_7 ($M = Nb, Ta$; $X = Cl, Br, I$; $Y = S, Se, Te$).⁷² Metal atoms occupy $\frac{3}{4}$ octahedral holes in alternating layers of anionic eutactic arrays and form M_3 triangles, which need 6 valence electrons for saturated metal-metal bonds. This electronic requirement is met precisely by the chalcogenide-halides M_3YX_7 ; the niobium halides Nb_3X_8 have one additional electron and are paramagnetic. The triply bridging ligand (X for the binaries; Y for the ternaries) of each M_3 triangle is pushed upward from its anionic plane. This effect, although refined by X-ray diffraction data, was nicely observed by atomic force microscopy on samples extracted from Ta_3TeI_7 .

(54) Trigonal Prismatic Coordination: The coordination chemistry of d^1 and d^2 metal ions includes trigonal prismatic as an alternative to octahedral environments. An important example is molybdenite MoS_2 , which has lubricating properties like graphite because MoS_2 layers are held together by van der Waals forces. The most stable form 2H- MoS_2 consists of two MoS_2 layers per unit cell, stacked according to $\cdots BcB CaC \cdots$, but there is also a 3R- MoS_2 polytype. In each layer, two close packed planes of S atoms are stacked in an eclipsed manner, which creates two sets of trigonal prismatic holes, but only one set is filled by d^2 Mo(IV) ions. There is weak Mo \cdots Mo bonding within the triangles that are not capped by S atoms, but it is insufficient to distort the plane of Mo atoms.⁷³ Similar layers occur for d^1 systems like $NbSe_2$ and $TaSe_2$, but they have different structural properties than MoS_2 . At low temperatures, Nb atoms shift slightly to give a 2×2 superstructure of $NbSe_2$ in the *ab*-plane.⁷⁴ The distortion of these Nb planes is an example of a *charge density wave* (“cdw”), which expresses the variation in bonding electron density within an extended structure.⁷⁵ Charge density waves can be commensurate (periodic) or incommensurate with the smallest unit cell and can lead to interesting transport properties. Although the dichalcogenides of Ta also exhibit CDWs, one polytype contains alternating layers of octahedral and trigonal prismatic coordinated Ta.⁷⁶

Layered compounds can undergo *intercalation*, which is the chemical process of introducing species into the van der Waals layers. Intercalating neutral molecules simply enlarges the separation between the layers than occurring in the original compound, whereas ionic species will either reduce (as cations) or oxidize (as anions) the original layer. MoS_2 reacts with n-butyl lithium, which intercalates Li^+ cations into the van der Waals layers and reduces each MoS_2 layer leading to $LiMoS_2$ with d^3 Mo(III), which prefers octahedral over trigonal prismatic coordination.⁷⁷ Thus, intercalation of Li^+ cations into MoS_2 also causes a topotactic reaction by shifting planes of S atoms relative to one another in each MoS_2 layer to create distorted octahedral coordination at each Mo site.

⁷² G.J. Miller, *J. Alloys Compds.* **1995**, 229, 93-106; M.D. Smith, G.J. Miller, *J. Am. Chem. Soc.* **1996**, 118, 12238-12239.

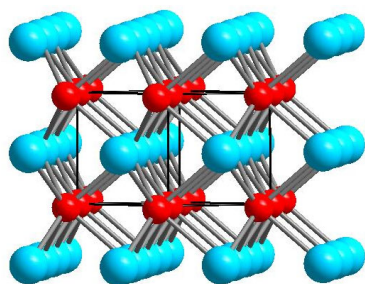
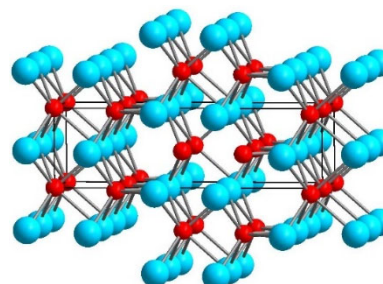
⁷³ K.A. Yee, T. Hughbanks, *Inorg. Chem.* **1991**, 30, 2321-2328.

⁷⁴ M. Marezio, P.D. Dernier, A. Menth, G.W. Hull, *J. Solid State Chem.* **1972**, 4, 425-429.

⁷⁵ C.D. Malliakas, M.G. Kanatzidis, *J. Am. Chem. Soc.* **2013**, 135, 1719-1722.

⁷⁶ B.E. Brown, D.J. Beerntsen, *Acta. Cryst.* **1965**, 18, 31-36.

⁷⁷ V. Petkov, S.J.L. Billange, P. Larson, S.D. Mahanti, T. Vogt, K.K. Rangan, M.G. Kanatzidis, *Phys. Rev. B* **2002**, 65, 0921051-0921054.

WC-Type (*c*-axis is vertical)NbAs-Type (*c*-axis is horizontal)

Among 3-d extended structures, there are two principal structure types involving trigonal prismatic coordination at both the cations and anions: (i) WC-type, space group $P\bar{6}m2$; and (ii) NbAs-type, space group $I4_1md$. Most examples of these structures involve d^2 metal cations. Because three faces of a trigonal prism are rectangular, these two structure types differ by the relative orientations of the trigonal prisms surrounding each metal atom – one set of rectangular faces become square faces in the NbAs-type.

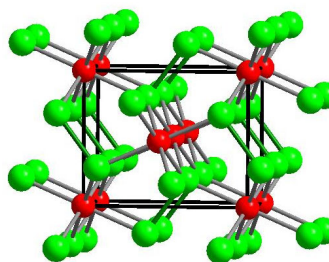
Nonmetal-Nonmetal Bonding: In metal-nonmetal or metal-metalloid compounds, bonding between the more electronegative component occurs if these atoms do not achieve a complete octet of valence electrons arising from electron donation by the electropositive metal atoms. There are two principal ways this effect can occur: (1) for transition metal compounds, the metals do not achieve sufficiently high oxidation states to completely reduce the nonmetal components; or (2) the composition of active metal cations does not provide the number of valence electrons sufficient to completely reduce the nonmetal components.

(55) Transition Metal Dichalcogenides: To prevent chalcogen–chalcogen bonds in these compounds, each metal atom must donate four valence electrons to the nonmetal atoms. But, the divalent state M(II) is common for all transition metals. Therefore, a plot of 3rd + 4th ionization potentials ($I_3 + I_4$) vs. group number provides some useful insights. Because the effective nuclear charges of atoms increase left-to-right across each period while atomic sizes increase down each group, the plots of ($I_3 + I_4$) increase with increasing group number for each period of transition metals, but they steadily decrease in value from 3d to 4d to 5d metals. Thus, forming the tetravalent state is energetically less costly for the earlier transition metals in a series and costlier for the later metals.

Metal *dioxides* typically form rutile-type structures with trigonal planar coordination at O atoms and no O–O bonding. The structures of metal *disulfides*, *diselenides*, and *ditellurides*, on the other hand, show changes from metal-metal bonding to nonmetal-nonmetal bonding by progressing left-to-right across the series of transition metals. Dichalcogenides with metals from groups 4-6 adopt layered CdI₂- or MoS₂-type structures, which show metal-metal bonding for electronic configurations d^1 - d^3 , as shown in slides #52-54. The *c/a* ratios for these CdI₂-types are ~1.6, which is close to the ideal value for HCP anion packing. Late metal ditellurides such as NiTe₂ and IrTe₂ have *c/a* = ~1.4, which suggests some degree of Te···Te attractions stronger than van der Waals interactions between the CdI₂-type layers. Electronic structure calculations suggest that Te is not fully reduced to Te²⁻ for the more electronegative transition metals Ni and Ir.⁷⁸ As a result, these examples belong to the BaSi₂-type family, also with space group $P\bar{3}m1$.

⁷⁸ S. Jobic, P. Deniard, R. Brec, J. Rouxel, *Z. anorg. allg. Chem.* **2004**, 598, 199-215.

The more prolific structure type among the diselenides, and ditellurides of the late transition metals is the cubic pyrite (FeS_2)-type, space group $Pa\bar{3}$ and symbol $cP12$. Fe atoms and disulfide groups adopt (NaCl)-type structure with the four disulfide groups cell oriented along each of the four body-diagonal. Pyrite-type FeS_2 is semiconducting, which supports formulation $\text{Fe}^{2+}(\text{S}_2)^{2-}$; the S–S distance is 2.162 Å. Pyrite-type FeS_2 also adopts another polymorph, called *marcasite*, space group $Pn\bar{m}$. Like pyrite-type FeS_2 , marcasite-type FeS_2 is semiconducting with disulfide groups but a slightly longer S–S distance of 2.217 Å. The marcasite structure is a distortion of the orthorhombic CaCl_2 -type structure (see slide #46) by tilting each octahedral coordination polyhedron toward the longest crystal axis (b), which creates short anion–anion (disulfide) distances.



Marcasite-Type FeS_2

disulfides, metals is Pearson a halite in each unit directions. its Iron marcasite,

(56) Zintl Phases: This broad family of compounds consists of polyanionic networks, fragments, or clusters of main group metalloids or nonmetals embedded in alkali or alkaline-earth metal cations.⁷⁹ Most of these compounds are semiconducting or semimetallic, which implies that their chemical structures are electronically precise, i.e., the number of valence electrons for the polyanion fills all bonding and nonbonding orbitals. Many of these structures obey the $8-N$ rule, where N is the number of valence electrons assigned to the metalloid or nonmetal component and $8-N$ is the connectivity of this atom to other like atoms. Such compounds were first extensively studied by E. Zintl in Darmstadt, Germany by carrying out reactions using liquid ammonia as a solvent. W. Klemm proposed the analogy between the structure of a polyanion and the isoelectronic element. From this, the Zintl-Klemm concept was born.

Examples of Zintl phases generally feature metalloids from groups 13-16 with alkali or alkaline-earth metals acting as the cations. The negative charge of the main group polyanion is determined by all valence electrons provided by the active metal component. To demonstrate the Zintl-Klemm concept, some illustrative 1:1 compounds include:

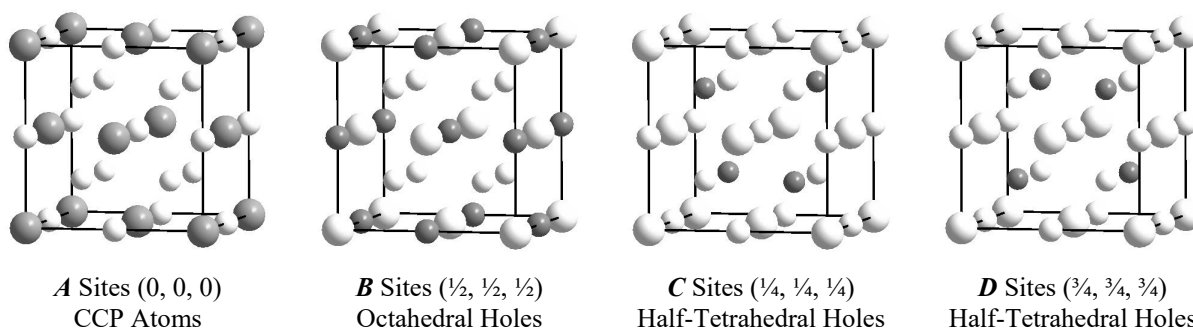
- NaTl-Type: Space group $Fd\bar{3}m$ ($cF16$); Tl^- , with 4 valence electrons, forms a diamond-like, 4-bonded tetrahedral network. Binary examples include LiAl and NaIn and avoid the larger alkali cations K^+ , Rb^+ , or Cs^+ . Isoelectronic diamond-like nets also occur for “half-Heusler” alloys such as LiAlSi, LiAlGe, LiAlSn, and NaInSn with half of the cation sites of the NaTl-type vacant.
- NaSn-Type: Space group $I4_1/acd$ ($tI64$); Sn^- , with 5 valence electrons, forms tetrahedral clusters $(\text{Sn}_4)^{4-}$, which resemble P_4 tetrahedra in white phosphorus. Most examples involve the larger alkali metals K, Rb, and Cs with Sn and Pb.
- LiSi-Type: Space group $I4_1/a$ ($tI32$); Si^- , with 5 valence electrons, forms a 3-bonded 3-d net based on inter-connected, four-fold symmetric spirals. Although there are no elemental analogues of this 3-bonded net, a different kind of 3-bonded net of four-fold symmetric spirals occur in SrSi_2 and BaSi_2 .

⁷⁹ *Chemistry, Structure, and Bonding of Zintl Phases and Ions*, Ed. S.M. Kauzlarich, Wiley-VCH, Heidelberg, 1996.

LiAs-Type: Space group $P2_1/c$ ($mP16$); As^- , with 6 valence electrons, forms a 2-bonded polymer based on four-fold symmetric spirals. The isoelectronic elements Se and Te form 2-bonded polymers based on three-fold symmetric spirals.

To complete the series, the hexagonal Li_2O_2 -Type of Na_2Se_2 , space group $P6_3/mmc$ ($hP8$) with $(Se_2)^{2-}$ units and cubic halite-type $LiCl$ with isolated Cl^- ions also follow the 8- N rule but are not generally considered Zintl phases.

(57) BCC Packing: Solid-state chemists often search for structure-building patterns that establish relationships among various structures. For example, the Heusler alloys, such as Cu_2MnAl , constitute an important intermetallic structure type that is closely related to the body-centered cubic sphere packing. Cu_2MnAl , space group $Fm\bar{3}m$ and Pearson symbol $cF16$, can be described as CCP Al atoms with Mn in all octahedral and Cu in all tetrahedral holes. The face-centered cubic unit cell contains four environments specified along the body-diagonal of the cubic cell:



Therefore, this structure involves four interpenetrating FCC arrangements of atoms and leads to numerous important structure types, depending on how the four different sites are decorated:

BCC: If all atoms are identical, this structure is none other than BCC packing, in which every atom is surrounded by 14 neighbors with 8 nearest neighbors forming a cube and 6 next nearest neighbors outside each face of the cube. Among the elements, the BCC structure occurs for some alkali metals and for transition metals from groups 5 and 6 like Nb and Mo. Furthermore, many elements transform to BCC before melting.

Heusler Alloys: This extensive set of ternary intermetallic compounds contains more than 1000 members comprising elements from most of the periodic table. They were discovered in the early 1900's and Cu_2MnAl surprisingly showed ferromagnetism, i.e., spontaneous magnetization, although none of the component elements is ferromagnetic. As a result, these compounds have been important for research on magnetism. Binary intermetallic examples include Fe_3Al and Mg_3Ln (Ln = lanthanide metal) in which the minority component is assigned to the **A** sites. Valence electron precise cases are the alkali metal pnictides A_3Pn such as Li_3Bi . "Full Heusler" compounds " X_2YZ ", space group $Fm\bar{3}m$ ($cF16$), generally place the X atoms in the **C** and **D** sites. In addition to their importance for magnetism, full Heusler compounds show significant emerging or multifunctional properties, such as superconductivity, topological edge states, thermoelectric behavior, magneto-optical, and magnetocaloric responses.⁸⁰

CsCl-Type: This ordered, binary derivative of BCC packing, space group $Pm\bar{3}m$ ($cP2$), occurs for a small set of ionic solids comprised of large alkali metal cations with halides as well as for

⁸⁰ T. Graf, C. Felser, S.S.P. Parkin, *Prog. Solid State Chem.* **2011**, 39, 1-50.

numerous intermetallic compounds. Three important families of CsCl-type binary intermetallic compounds include: (i) early-late transition metal compounds having ~ 6 valence d , s , and p electrons per atom, e.g., TiFe, ZrRu, YRh, LnAg, LnCd (Ln = lanthanide); (ii) semiconducting alkali metal-gold compounds CsAu and RbAu; and (iii) Hume-Rothery compounds such as CuZn (β -brass) and NiAl with ~ 1.5 valence s and p electrons per atom comprising elements from groups 10-14.

NaTl-Type: These 1:1 Zintl phases involving alkali metals and metals from groups 12 and 13 exhibit another distribution of elements in BCC packing, which gives rise to a diamond-type covalent network of the more electronegative component. These compounds are semiconducting or semimetallic.

Additional structure types emerge from this BCC packing model if vacancies are included:

Fluorite-type: These AX_2 or A_2X structures arise when the **B**-site “octahedral” voids in CCP packing (**A**-site A atoms in AX_2 or X atoms in A_2X) are vacant. The minority component has an 8-coordinate cubic environment. Many examples are ionic solids involving either very large cations with small anions such as actinide dihydrides AnH_2 and dioxides AnO_2 or small cations with large anions such as Li_2O and Na_2Te . Some intermetallic compounds like semiconducting Mg_2Sn and Al_2Au (the “purple plague”) also adopt this structure type. Al_2Au forms at the interface between gold and aluminum in certain microelectronics and disrupts these electrical contacts because it has a significantly larger resistivity than gold.

Half-Heusler alloys:⁸¹ This impressive class of ternary compounds have potential for emerging energy applications and spintronics. Examples containing 8 or 18 valence electrons per formula unit are semiconducting with bandgaps that can be “tuned” between 0 and 4 eV just by revising the electronegativity differences among the constituent elements. Their structures are described as a “fusion” of NaCl-type and sphalerite (zinc blende) ZnS-type so that correctly assigning the position of elements is important to understand their properties. The following table⁸¹ includes various examples with the most electronegative element assigned to the **A**-site:

Composition	a (Å)	# e^-s	A -site	B -site	C -site	D -site	“NaCl”	“ZnS”
LiMgN	4.910	8	N		Mg	Li	LiMg	MgN
LiAlSi	5.928	8	Si		Al	Li	LiAl	AlSi
TiCoSb	5.884	18	Sb	Ti	Co		TiSb	CoSb
MgCuSb	6.168	18	Sb	Mg	Cu		MgSb	CuSb
MgAgAs	6.210	18	As		Ag	Mg	MgAg	AgAs
LuAuSn	6.565	18	Sn	Lu	Au		LuSn	AuSn

Although all examples are derived from the fluorite-type, “normal” half-Heusler compounds are considered to have the most electronegative and electropositive components form the “NaCl” substructure. The 8-electron examples are also called Nowotny-Juza phases.

(58) HCP Packing (Trigonal Pyramidal Voids): In HCP, two tetrahedral voids share a common face and create a single trigonal bipyramidal (tbp) void, which lies in the planes of the close packed atoms. As a result, there is one tbp void per atom forming the HCP array. If the HCP stacking is

⁸¹ F. Casper, T. Graf, S. Chadov, B. Balke, C. Felser, *Semicond. Sci. Technol.* **2012**, 27, 063001.

given as $\dots BC\dots$, then the tbp centers are located at the c positions in the B layers, and at the b positions in the C layers. The shape of the trigonal bipyramid is determined by the c/a value of the HCP packing. For $c/a = 1.633$, the ideal value, the ratio of axial to equatorial distances between the center of a tbp void and an HCP atom is $\sqrt{2}$ (1.41), which is much larger than distances observed in tbp molecules like PF_5 (1.04) and PCl_5 (1.06). Therefore, when the tbp voids are occupied, the c/a values are generally much smaller than the ideal value for HCP. One example observed for numerous intermetallic compounds is the Ni_2In -type structure, space group $P6_3/mmc$ ($hP6$), in which all tbp and octahedral voids of the HCP arrangement of In atoms are occupied by Ni atoms so that every In atom site is coordinated by 11 Ni atoms. The Ni_2In -type structure occurs for numerous transition metal-rich pnictides and tetrelides (elements from group 14) and their observed c/a values are ~ 1.20 – 1.25 , which set the axial-to-equatorial distance ratios at ~ 1.04 – 1.08 . Some binary systems, such as Mn_{2-x}Sb and Ni_{2-x}Sn , have vacancies on the tbp sites. In these cases, if $x = 1$, the NiAs-type emerges so that these defect structures may be described as either “stuffed” NiAs-type or “defect” Ni_2In -type.

Each plane of close packed and tbp atoms together creates a plane of 3-bonded atoms in a honeycomb net, designated by its Schläfli symbol 6^3 , which means that three hexagons meet at every node (atom site). The structures of hexagonal BN and graphite consist of such honeycomb planes that are held together by relatively weak van der Waals interactions. Boron and gallium also adopt planar 6^3 nets in superconducting MgB_2 , metallic AlB_2 , as well as LnB_2 and LnGa_2 (Ln = lanthanide metal). In this AlB_2 -type structure, space group $P6/mmm$ ($hP3$), the honeycomb nets are stacked in an eclipsed manner and the larger metal atoms occupy the 12-coordinate hexagonal prismatic sites between these planes. From a different perspective, these diborides and digallides can be derived from the Ni_2In -type: the HCP and tbp sites contain the majority component (B or Ga) while the HCP octahedral holes have the minority component (Mg, Al, or Ln). The unit cell contains just one 6^3 layer with c/a values ~ 1.1 – 1.2 for diborides and ~ 0.96 for digallides. These values correspond to Ni_2In -type c/a values ~ 1.9 – 2.4 so that the 6^3 nets are widely separated relative to the intraplanar B–B or Ga–Ga distances within the nets. Ternary derivatives of the AlB_2 -type include ZrBeSi ($c/a \sim 1.9$) and LnCuSi ($c/a \sim 1.7$, for LuCuSi , ~ 1.9 for LaCuSi).

(59) The “Coloring” Problem:^{82,83} The examples presented in slides **(57)** and **(58)** demonstrate the diversity offered by 3-d extended structures as the number of different elements increases. For example, the structures of TiFe and NaTl are two different ways of “coloring” BCC packing by two elements in equal numbers. The “coloring” problem is phrased by the following question: *Given a network of atoms and several different types of atoms at a fixed chemical composition, what is the best way to decorate (“color”) the network with these atoms?* The optimum structure for a specified stoichiometry corresponds to the overall lowest total energy.

Various characteristics of the different elements, such as valence electron counts, relative electronegativities, or relative sizes, will influence the optimal distribution pattern of the different elements. Another example derived from BCC sphere packing is a comparison between cubic CsCl-type TiFe and tetragonal TiCu. Along c , (001) planes of atoms follow a $\dots\text{Ti-Ti-Cu-Cu}\dots$ sequence in TiCu, whereas it is $\dots\text{Ti-Fe-Ti-Fe}\dots$ in TiFe. TiFe and TiCu differ in the average

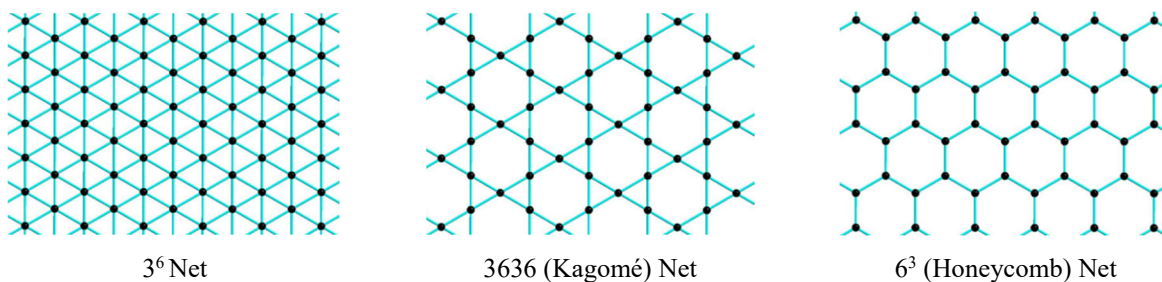
⁸² J.K. Burdett, S. Lee, T. J. McLarnan, *J. Am. Chem. Soc.* **1985**, *107*, 3083-3089.

⁸³ G. J. Miller, *Eur. J. Inorg. Chem.* **1998**, 523-536.

number of valence d electrons per atom, which means that filling electronic states influences their respective structures.

Analysis of electronic energy calculations for molecules and solids identify two energetic components contributing to the optimal “coloring” of any network: a site-energy term and a bond-energy term.⁸³ The site energy is related to Gimarc’s *topological charge stabilization*,⁸⁴ which argues that the more electronegative component of a molecule tend to occupy positions of low coordination number. An interesting example of this concept is comparison between realgar As_4S_4 and tetrasulfur tetranitride S_4N_4 . The two molecules adopt the same skeleton with four 2-bonded sites and four 3-bonded sites. Since electronegativities increase from As to S to N, S takes the 2-bonded sites in As_4S_4 but the 3-bonded sites in S_4N_4 . The bond-energy term is important for $\text{Ta}_{1.05}\text{Nb}_{0.95}\text{S}$,⁸⁵ for which H.F. Franzen described the concept of *differential fractional site occupancy*.⁸⁶ This tetragonal metal-rich compound is constructed of 6-layer S-M'-M-M'-S slabs. Although the metal composition is nearly equimolar, the inner M sites of the slab prefer Ta and the outer M' sites of the slab prefer Nb. This unequal metal atom distribution argues for bond-energy influences because the cohesive energy of Ta exceeds that of Nb.

(60) Networks: Describing structures as networks emphasizes bonds between atoms and coordination geometry. An important aspect of networks, though, is the occurrence of rings by counting the number of atoms or bonds that form a loop.^{87,88} Consider the planar borocarbide networks in CaB_2C_2 and ScB_2C_2 . In each structure, the B and C atoms are each 3-connected. In CaB_2C_2 , the $[\text{B}_2\text{C}_2]$ net contains only 4- and 8-membered rings, i.e., only even-membered rings. This net can be designated by its Schläfli symbol 48^2 because every atom (node) is surrounded by one 4-ring and two 8-rings. In ScB_2C_2 , the $[\text{B}_2\text{C}_2]$ net contains 5- and 7-membered rings, i.e., only odd-membered rings, and is designated by $(5^27)(57^2)_3$. As a result of this “topology”, the 48^2 net can be decorated by two different elements in an alternating pattern – this is called a bipartite net. On the other hand, the $(5^27)(57^2)_3$ net cannot completely separate the two different elements. There must be homoatomic bonds. Another sequence of examples is the 2-d closed packed 3^6 net, the 3636 kagomé net, and the honeycomb 6^3 net. The graphene-type 6^3 net can be bipartite as seen in BN, whereas the other two, which include 3-membered rings, cannot.



If atoms building networks have unpaired electrons and show local magnetic moments, then bipartite networks can accommodate antiferromagnetic ordering. Any non-bipartite net, however, creates frustration. The kagomé net is an important model for quantum materials.

⁸⁴ B.J. Gimarc, *J. Am. Chem. Soc.* **1983**, *105*, 1979-1984.

⁸⁵ X. Yao, G.J. Miller, H.F. Franzen, *J. Alloys Compd.* **1992**, *183*, 7-17.

⁸⁶ H.F. Franzen, M. Köckerling, *Prog. Solid State Chem.* **1995**, *23*, 265-289.

⁸⁷ J.K. Burdett, S. Lee, *J. Am. Chem. Soc.* **1985**, *107*, 3063-3082.

⁸⁸ S. Lee, L. Hoistad, *J. Alloys Compds.* **1995**, *229*, 66-79.

(61) Perovskites: (READING: Wells, pp. 179-186, 578-589) An especially important class of inorganic structures for their physical and chemical properties is the *perovskites*, which have the general formula ABX_3 . They are most numerous for oxides, i.e., $X = O$, but also exist among halides, sulfides, and nitrides. Complex oxides having the general formula ABO_3 can adopt two different and broad structure types depending on the cation sizes:

- If the size of cation $A \approx$ size of cation B , both of which are smaller than the size of O^{2-} , structures will be related to corundum Al_2O_3 or ilmenite $TiFeO_3$ by having close packed oxide ions with A and B cations in octahedral holes; or
- If the size of cation $A \approx$ size of O^{2-} and cation B is smaller, then perovskite structures like cubic $CaTiO_3$ or hexagonal $BaNiO_3$ form from stackings of AO_3 close packed planes.

Perovskites are built of close packed AX_3 planes with no $A-A$ nearest neighbors. To minimize $A \cdots A$ repulsions in 3-d space, these layers stack so that A atoms sit over X_3 triangles to create one $[X_6]$ and three $[A_2X_4]$ octahedral holes for every AX_3 formula unit. B atoms fill the X_6 octahedra to give the empirical formula ABX_3 . Analysis of the various stacking possibilities of AX_3 eutactic planes shows that BX_6 octahedra can only share vertices or faces, so that each X atom is shared between two BX_6 octahedra.

CCP-type ($\cdots ABC \cdots$) stacking of AX_3 planes leads to cubic $CaTiO_3$ -type perovskites with only vertex-sharing $[TiO_{6/2}]$ octahedra and linear $Ti-O-Ti$ angles. If the A cation sites are empty, the outcome is the cubic ReO_3 -type with linear $Re-O-Re$ angles. On the other hand, HCP-type ($\cdots AB \cdots$) stacking of AO_3 planes leads to hexagonal $BaNiO_3$ -type perovskites with only face-sharing $[NiO_{6/2}]$ octahedra, which form chains of Ni atoms (Ni-Ni distance is 2.40 Å) and nonlinear Ni-O-Ni angles. Although the Ni-Ni distances are short, $BaNiO_3$ is an electrical insulator because Ni(IV) with a d^6 configuration is closed shell for an octahedrally coordinated transition metal. There are numerous other perovskite-type *polytypes*, which arise by various stacking patterns of the AX_3 planes.

(62) The structures of cubic perovskites ABX_3 with linear $B-X-B$ bridges often distort to give nonlinear $B-X-B$ angles. Reasons for these distortions include both geometrical and electronic factors:

- Geometrical Factors:** The formula ABX_3 can be analyzed using ionic radii by a *tolerance factor* t , which establishes the allowed (“tolerated”) relationship between $A-X$ distances and $B-X$ distances for linear $B-X-B$ angles:

$$t = \frac{(R_A + R_X)}{\sqrt{2}(R_B + R_X)}.$$

For cubic perovskites, where the coordination environment of each A cation is a cuboctahedron of 12 X atoms, these factors vary between 0.9 and the ideal value of 1.0. If the A cation is too small so that $t < 0.9$, then icosahedral coordination at the A site becomes preferred and the $B-X-B$ bridges are nonlinear. $CaCu_3Ge_4O_{12}$, space group $Im\bar{3}$, is one example with A site cations Ca^{2+} and Cu^{2+} and B site cations are Ge^{4+} .⁸⁹ Although the Ca^{2+} and Cu^{2+} cations are relatively small, they are significantly larger on average than Ge^{4+} so that the perovskite network distorts because the tolerance factor becomes too low. The GeO_6 octahedra remain nearly regular and tilt so that each Ca^{2+} cation is icosahedrally coordinated and each Cu^{2+} is nearly square planar coordinated. The resulting $Ge-O-Ge$ angle is 143.7° . Another example is $GdFeO_3$ with $Fe-$

⁸⁹ Y. Osaki, M. Ghedira, J. Chenavas, J.C. Joubert, M. Marezio, *Acta Cryst. Sect. B* **1977**, B33, 3615-3617.

O–Fe angles of 145.4° and 148.3° .⁹⁰ If the tolerance factor approaches 0.71, then *A* and *B* cations have similar sizes, and the ilmenite structure occurs (see above). On the other hand, if the tolerance factor exceeds 1.0, then hexagonal perovskites like BaNiO₃-type are preferred.

- (b) Electronic Factors: Bending the *B–X–B* bridges can also occur to reduce *B–X* π -antibonding interactions for linear *B–X–B* bridges. This effect is often more evident when the *A* cation site is vacant, such as observed for the sequence of transition metal trifluorides from NbF₃ to RhF₃.⁹¹ Cubic NbF₃ is isostructural with ReO₃ having a 3-d network of vertex-sharing [NbF_{6/2}] octahedra and linear Nb–F–Nb angles. Rhombohedral RhF₃, on the other hand, has the same connectivity of [BF_{6/2}] octahedra as in the cubic structure, but all Rh–F–Rh linkages are bent because of rotating one [RhF₆] octahedron. If this one octahedron is rotated clockwise, then all surrounding octahedra are necessarily rotated counterclockwise and the sequence continues resulting in the rhombohedral FeF₃-type structure, space group $R\bar{3}c$ (*hR8*). By progressing from *d*² NbF₃ to *d*⁶ RhF₃, the *t*_{2g} orbitals of the octahedrally coordinated metals become increasingly filled. Since these orbitals are metal-ligand π -antibonding in the trifluorides, bending at the bridging fluoride ligands reduces the metal-fluoride antibonding interaction. This electronic effect also explains the change from linear CO₂ to nonlinear O₃.

(63) SUMMARY: Atomic structure plays a central role in the characterization of any solid-state compound. The principles utilized by solid-state chemists utilize a variety of geometrical and chemical concepts. As chemists, valence electron counting coupled with an understanding of simple geometrical shapes provide much useful information. In this unit, we discussed

- Structure descriptions utilize the mathematical concepts of sphere packings and graph theory. The packing of atomic spheres is characterized by the efficiency of filling space with spheres as well as the sizes of void spaces, as measured by radius ratios. The theory of graphs identifies atomic structures with networks in which each node is an atomic site. These descriptions are helped by symmetry for crystalline structures. Space groups, unit cell parameters, and atoms of the asymmetric unit provide the information to generate the complete crystal structure, for which the *International Tables of Crystallography, Volume A* is a helpful resource.
- Element characteristics that influence structure include numbers of valence electrons, relative electronegativities, and atomic or ionic sizes. Valence electron counting rules, such as the Octet Rule for main group compounds, the 18-electron rule for transition metal centers, Wade-Lipscomb rules for boron-related cages, among various others are frequently invoked. Electronegativity differences between two elements determine the nature of their bonding interactions from ionic to covalent. Also, crystal structure analysis yields interatomic distances from which various atomic or ionic radii can be evaluated.
- Structure-building principles generally involve coordination environments, which include both the number of ligands and the geometry. Because solids consist of Avogadro numbers of atoms, the presence of structural imperfections such as vacancies or interstitial atoms can arise, whether by enthalpic or entropic reasons. In compounds, the strongest interactions are typically metal–nonmetal bonds, which can range from polar-covalent to

⁹⁰ P. Coppens, M. Eibschuetz, *Acta Cryst.* **1965**, 19, 524-531.

⁹¹ J. Lin, G.J. Miller, *Inorg. Chem.* **1993**, 32, 1476-1487.

ionic interactions. In addition to these and depending on valence electron counts, metal–metal or nonmetal–nonmetal bonds can arise.

- Solid state chemists keep several important structure types at hand because they provide certain fundamental geometrical and chemical characteristics. The metallic elements show FCC, HCP, and BCC packings, while the main group elements form covalently bonded networks that decrease in connectivity as the valence electron count increases. Among the simplest chemical compositions for compounds, many 1:1 structure types vary from 4-bonded sphalerite (zinc blende) or wurtzite types, including the Zintl compound sodium thallide, 6-bonded halite or nickel arsenide types, to 8-bonded cesium chloride. 1:2 structure types include rutile, layered cadmium dihalides, pyrite, and the “intermetallic” dinickel indium and aluminum diboride types. Lastly, perovskites represent an important structure class ranging from cubic to hexagonal forms.

Three important structural classes that were not specifically discussed in this unit include:

Superconducting $\text{YBa}_2\text{Cu}_3\text{O}_{7-\delta}$, space group $Pmmm$ ($hP13$) contains two $[\text{CuO}_{4/2}]$ layers surrounding Y^{3+} cations and one $[\text{CuO}_2\text{O}_{2/2}]$ chains. Two Ba^{2+} cations are encapsulated by the cuprate chains and layers. Cu atoms in the layers are 5-coordinate by 4 O atoms in the layer and 1 O atom from the chains. Oxygen vacancies occur preferentially first at O atom sites in the chains and then in the layers.

Ruddleston-Popper phases are formulated as $A_{n+1}B_nX_{3n+1}$, such as Sr_2RuO_4 and $\text{Sr}_3\text{Ru}_2\text{O}_7$. $\text{La}_{2-x}\text{Sr}_x\text{CuO}_4$ belongs to this class of compounds and was responsible for igniting intense study of superconducting cuprates beginning in the mid-1980's. This compound consists $[\text{CuO}_2\text{O}_{4/2}]$ layers of vertex-sharing octahedra. The axial Cu–O distances are somewhat longer, by ~ 1.25 than the equatorial Cu–O distances.

The ThCr_2Si_2 -type structure describes a vast collection of ternary intermetallic compounds.⁹² ThCr_2Si_2 is tetragonal with the large Th atoms at unit cell corners and center surrounded by Si–Si dimers oriented along c . The arrangement of these dimers creates tetrahedral voids filled by the Cr atoms to create $[\text{CrSi}_{4/4}]_2$ layers of edge-sharing tetrahedra. Depending on the chemical composition and valence electron counts, distances within the dimer units can be very long. Also, the various metals occupying Cr sites can lead to interesting transport and magnetic properties.

Some Additional References:

1. P. M. Adams, *Inorganic Solids*; Wiley: Chichester, 1974.
2. G. Burns and A. M. Glazer, *Space Groups of Solid State Scientists*, Academic Press, 1990.
3. G. M. Clark, *The Structure of Non-Molecular Solids*; Applied Science: London, 1972.
4. J. Donahue, *The Structures of the Elements*, Krieger Publishing Co., Malabar, FL, 1982.
5. F. Hulliger, *Structural Chemistry of Layer-Type Phases*, Reidel, 1976.
6. B. G. Hyde, S. Andersson, *Inorganic Crystal Structures*; Wiley: New York, 1989.
7. U. Müller, *Inorganic Structural Chemistry*, Wiley, 2nd Edition, 1993.
8. M. O’Keeffe and B. G. Hyde, *Crystal Structures, I. Patterns and Symmetry*, Mineral. Soc. America, 1996.
9. R. W. G. Wyckoff, *Crystal Structures* (all volumes); Interscience: New York, 1963.

⁹² M. Shatruk, *J. Solid State Chem.* **2019**, 272, 198-209.